Fermi National Accelerator Laboratory

FERMILAB-Conf-80/47-EXP
7160.451

A-DEPENDENCE OF INCLUSIVE HADRON SCATTERING AT 100 GeV*

A. E. Brenner, D. C. Carey, J. E. Elias,
P. H. Garbincius, and V. A. Polychronakos
Fermi National Accelerator Laboratory, Batavia, Illinois 60510 USA

and

D. Cutts, R. S. Dulude, B. W. Hughlock,
R. E. Lanou, Jr., and J. T. Massimo
Brown University, Providence, Rhode Island 02912 USA

and

M. T. Chiaradia, C. Demarzo, C. Favuzzi, G. Germinario,
L. Guerriero, P. LaVopa, G. Maggi, F. Posa, G. Selvaggi,
P. Spinelli, and F. Waldner
Istituto di Fisica and Istituto Nazionale di Fisica Nucleare, Bari, Italy

and

D. S. Barton, G. W. Brandenburg, W. Busza, T. Dobrowolski,
J. I. Friedman, C. Halliwell, H. W. Kendall, T. Lyons,
B. Nelson, L. Rosenson, and R. Verdier
Massachusetts Institute of Technology, Cambridge, Massachusetts 02139 USA

and

J. Nassalski, T. Siemiarczuk, and I. P. Zielinski
Institute of Nuclear Research, Warsaw, Poland

June 1980

*Submitted to the XX International Conference on High Energy Physics, Madison, Wisconsin, July, 1980

A-DEPENDENCE OF INCLUSIVE HADRON SCATTERING AT 100 GeV

A.E. Brenner, D.C. Carey, J.E. Elias, P.H. Garbincius, and V.A. Polychronakos[a]
Fermi National Accelerator Laboratory, Batavia, Illinois 60510

and

D. Cutts, R.S. Dulude, B.W. Hughlock, R.E. Lanou, Jr., J.T. Massimo
Brown University, Providence, Rhode Island 02912

and

M.T. Chiaradia, C. Demarzo, C. Favuzzi, G. Germinario, L. Guerriero, P. LaVopa, G. Maggi, F. Posa, G. Selvaggi, P. Spinelli, and F. Waldner
Istituto di Fisica and Istituto Nazionale di Fisica Nucleare, Bari, Italy

and

D.S. Barton[b], G.W. Brandenburg, W. Busza, T. Dobrowolski[c], J.I. Friedman, C. Halliwell[d], H.W. Kendall, T. Lyons, B. Nelson, L. Rosenson, and R. Verdier
Massachusetts Institute of Technology, Cambridge, Mass. 02139

and

J. Nassalski, T. Siemiarczuk, and I.P. Zielinski
Institute of Nuclear Research, Warsaw, Poland

ABSTRACT

We have performed an experiment to study the inclusive processes $a^+ + A \to c^\pm + X$, where a and c are either π, K, or p. The nuclear targets used were C, Al, Cu, Ag, and Pb. We have studied the Feynman x and p_T dependence of particle c using the Fermilab Single Arm Spectrometer. In this paper we present cross sections as a function of x at transverse momenta of 0.3 and 0.5 GeV/c for each target nucleus. The A-dependence is parameterized as $\sigma_A = \sigma_o A^\alpha$, and the x-dependence of α is studied.

Submitted to the XX International Conference on High Energy Physics, Madison, Wisconsin, July 1980.

Pre ious hadron-nucleus (hA) experiments[1] have shown that at high energies the multiplication of hadrons within a nucleus is relatively weak. This is reflected in the observations that with increasing nuclear thickness, there is at most a linear increase in the multiplicity of the produced hadrons[2] and, in comparison with hadron-nucleon (hN) interactions, only a slight depletion in the production of the most energetic secondaries.[3] The mechanism by which newly formed hadrons (or their constituents) lose energy in, or interact with, nuclear matter is of fundamental interest. For this reason, we have performed an experiment to study the inclusive process $h + A \rightarrow h' + \chi$ where h was either π^+, K^+, or p; h' was either $\pi^\pm$, $K^\pm$, or p; and A, the nuclear target, was either C, Al, Cu, Ag or Pb. Previous measurements of the A-dependence of inclusive processes in the beam fragmentation region include proton interactions at 24 GeV,[4] Λ^0 production by protons at 300 GeV,[5] neutron production by protons at 400 GeV,[6] and of charged particles by neutrons above 100 GeV.[3]

This experiment was a continuation of an extensive study of the production of particles in hN interactions.[7] Since essentially the same equipment was used in the two experiments, an accurate comparison between hN and hA interactions, free of many systematic errors, is possible.

The experimental apparatus consisted of the Fermilab M6E beam line and the Single Arm Spectrometer Facility. An incident beam of 100 GeV/c was used. The production of the fast secondary, h', was measured over the Feynman x range $0.3 \lesssim x \lesssim 0.88$ and the transverse momentum range $0.18 \leq p_T \leq 0.5$ GeV/c. Data were taken simultaneously for the nine reaction types ($\pi\pi$, πK, πp, etc). The details of the instrumentation of the beam line and spectrometer have been summarized in Ref. 7. Good π-K-p separation was achieved over the entire kinematic range using the eight Cerenkov counters of the facility. A list of the targets used in the experiment is given in Table 1. In a manner similar to that described in Ref. 7, the interaction rates were corrected for particle absorption and decay in the spectrometer, finite target thickness, multiple scattering losses in the spectrometer, particle misidentification and track reconstruction inefficiencies. The corrected rates were then used to obtain, for every channel, the invariant differential cross section $E\,\frac{d^3\sigma}{dp^3}$ (mb/GeV^2 per nucleus).

The most significant features of the inclusive cross-sections are described in this paper. Complete numerical results and comparison with models as well as some information on the associated particle production will be published elsewhere.

In Figs. 1 and 2 we illustrate how $\frac{E}{A}\,\frac{d^3\sigma}{dp^3}$, i.e., the differential cross sections per nucleon, depend on x, p_T and A. The errors indicated are statistical. The overall normalization uncertainty is estimated to be 10%. The systematic uncertainty due to particle misidentification in the reactions with an outgoing kaon is less than 5%. The results shown are for channels where we have the highest statistics. The other channels exhibit similar trends.

To facilitate the presentation of all these data, we fitted the A-dependence of the cross sections to the empirical form

$$E\,\frac{d^3\sigma}{dp^3}\;(x,\,p_T,\,A) = \sigma_o(x,\,p_T)\;A^{\alpha(x,p_T)}\quad .$$

Hydrogen data were not included in the fits. The results are given in Table 2 and Fig. 3. For comparison our previous hydrogen differential cross sections are given both in Table 2 and Figs. 1 and 2.

The following general trends in the data should be noted.

1. Over the entire range of x covered in this experiment, the effectiveness of nucleons in the nucleus in producing particles decreases with A. This is true not only for channels where the outgoing particle is identical with the incoming one ($\pi^+ \to \pi^+$, $K^+ \to K^+$, $p \to p$), but also for channels where the outgoing particle is different (e.g., $\pi^+ \to \pi^-$). If one interprets this decrease of the effectiveness of nucleons in producing particles as an attenuation of the incident or outgoing state, a comparison of p and π -induced reactions shows that, independent of the produced particle, the attenuation is greater for incident protons.

2. In the range of p_T covered (180–500 MeV/c), no significant differences are seen in the A-dependence of particles produced with different p_T.

3. Comparison of our results for 100 GeV proton-induced reactions with the 24 GeV data of Eichten et al.[4] (see Fig. 3), suggest that there are no differences in the observed A-dependences over this energy range.

4. At the highest values of x the differential cross sections tend towards values which one would expect from the contribution of single collisions in the nucleus (i.e., primarily peripheral).[8] There is no evidence of high x cross sections per nucleon approaching hydrogen values as suggested by some parton-multi-peripheral models.[9]

5. The π–π data at high x is rather poorly represented by the A parameterization. There is a tendency for the cross section per nucleon to decrease with A faster than a simple power law.

6. In the π–π channel, in particular $\pi^+ \to \pi^-$, there is an enhancement at high x which has only a weak A-dependence. A possible interpretation is that many of the high x pions are from the decay of resonances coherently produced on the nucleus.

We would like to express our thanks to the many people at the Fermi National Accelerator Laboratory who have contributed to the successful operation of this experiment. This work was supported in part by the U.S. Department of Energy, the National Science Foundation Special Foreign Currency Program, and the Istituto Nazionale di Fisica Nucleare, Italy.

References

a. Present address: Brookhaven National Laboratory, Upton, N.Y. 11973.

b. Present address: Brookhaven National Laboratory, Upton, N.Y. 11973.

c. Present address: Centre d'Etudes Nucleaires de Saclay, Gif-sur-Yvette, France.

d. Present address: University of Illinois at Chicago Circle, Chicago, Illinois 60680.

1. For a review of hadron-nucleus collisions see, for example: W. Busza, Acta Phys. Pol. B8, 333 (1977); C. Halliwell, Proc. VIII Int. Symp. on Multiparticle Dynamics, Kaysersberg, 1977.

2. See for example: J.E. Elias et al., Phys. Rev. Lett. 41, 285 (1978).

3. See for example: D. Chaney et al., Physi. Rev. Lett. 40, 71 (1978).

4. T. Eichten et al., Nucl. Phys. B44, 333 (1972).

5. K. Heller et al., Phys. Rev. D16, 2737 (1977).

6. M.R. Whalley et al., Univ. of Michigan report UM-HE 79-14.

7. W.W. Toy, Ph.D. Thesis, M.I.T., 1978 (unpublished); W. Aithenhead, Ph.D. Thesis, M.I.T., 1979 (unpublished). D. Cutts et al., Phys. Rev. Lett. 40, 141 (1978); D. Cutts et al., Phys. Rev. Lett. 43, 319 (1979).

8. Private communication - Haifa group.

9. See for example: N. Nikolaev et al., CERN Preprint TH-2541 (1978).

TABLE 1

Targets used in this experiment. Most data was taken with thick targets; others were used for finite thickness correction.

Target	A	Thickness ($g\text{-}cm^{-2}$)
C	12.0	1.37
		3.93
		5.79
Al	27.0	5.99
Cu	63.5	2.89
		5.94
		9.94
Ag	107.9	6.71
Pb	207.2	2.06
		4.00
		7.38

TABLE 2

Results of fits: $E\,\frac{d^3\sigma_A}{dp^3} = \sigma_o\,A^{\alpha}$ and measured hydrogen cross section, $\sigma_H = E\,\frac{d^3\sigma_H}{dp^3}$. (from reference 7, previously unpublished)

Reaction	x	α	σ_o [mb/(GeV/c)^2]	σ_H
$\pi^+ \to \pi^+$, $p_T = .3$	.30	.65 ± .03	11.5 ± 1.2	6.36 ± .22
	.40	.66 ± .01	8.02 ± .41	5.15 ± .19
	.50	.58 ± .03	8.95 ± 1.04	4.50 ± .18
	.60	.60 ± .03	7.61 ± .85	4.34 ± .09
	.70	.63 ± .02	6.39 ± .38	4.29 ± .09
	.80	.59 ± .02	6.47 ± .51	4.35 ± .07
	.88	.50 ± .03	8.80 ± .91	4.94 ± .11
$p_T = .5$	.30	.66 ± .04	6.1 ± 1.1	3.58 ± .15
	.50	.62 ± .03	3.36 ± .39	1.91 ± .06
	.80	.51 ± .02	3.14 ± .27	1.60 ± .03
$\pi^+ \to \pi^-$, $p_T = .3$	.30	.70 ± .02	5.11 ± .47	3.52 ± .14
	.40	.64 ± .02	3.67 ± .34	2.02 ± .07
	.50	.59 ± .04	1.83 ± .25	1.11 ± .04
	.60	.67 ± .04	1.40 ± .20	0.97 ± .04
	.70	.66 ± .04	1.30 ± .18	0.83 ± .03
	.80	.65 ± .03	1.07 ± .13	0.65 ± .03
	.88	.54 ± .05	1.07 ± .20	0.46 ± .02
$p_T = .5$	.30	.63 ± .03	3.44 ± .38	1.76 ± .11
	.50	.64 ± .04	0.99 ± .16	0.67 ± .04
	.80	.57 ± .07	0.27 ± .07	0.14 ± .02
$\pi^+ \to K^+$, $p_T = .3$	.30	.58 ± .08	1.49 ± .48	0.66 ± .12
	.40	.69 ± .06	0.72 ± .18	0.49 ± .08
	.50	.65 ± .05	0.61 ± .14	0.38 ± .07
	.60	.66 ± .07	0.40 ± .11	0.23 ± .03
	.70	.58 ± .07	0.45 ± .12	0.22 ± .03

	x	α	σ_o	σ_H
$\frac{\pi^+ \to K^-}{p_T = .3}$	.30	.70 ± .09	0.64 ± .24	0.40 ± .07
	.40	.64 ± .09	0.49 ± .16	0.33 ± .04
	.50	.63 ± .12	0.24 ± .11	0.16 ± .02
	.60	.76 ± .08	0.11 ± .03	.103 ± .014
	.70	.69 ± .10	0.12 ± .05	.068 ± .010
$\frac{\pi^+ \to p}{p_T = .3}$	.30	.69 ± .06	1.27 ± .32	0.65 ± .07
	.40	.64 ± .04	0.93 ± .15	0.45 ± .06
	.50	.59 ± .05	0.63 ± .13	0.33 ± .05
	.60	.61 ± .09	.32 ± .12	0.17 ± .02
	.70	.59 ± .09	0.20 ± .06	0.11 ± .02
$p_T = .5$	.30	.75 ± .07	0.58 ± .16	0.43 ± .05
	.50	.66 ± .08	0.40 ± .12	0.19 ± .02
$\frac{p \to p}{p_T = .3}$	.30	.61 ± .02	10.1 ± 1.0	5.62 ± .29
	.40	.59 ± .02	11.4 ± 0.8	6.41 ± .33
	.50	.55 ± .02	13.3 ± 1.2	8.51 ± .39
	.60	.51 ± .02	15.5 ± 1.2	10.00 ± .20
	.70	.49 ± .02	18.2 ± 1.5	10.72 ± .21
	.80	.51 ± .01	16.4 ± 0.8	11.75 ± .17
	.88	.46 ± .01	20.0 ± 1.0	13.60 ± .27
$p_T = .5$	.30	.60 ± .03	6.0 ± 0.8	2.90 ± .18
	.50	.50 ± .08	8.8 ± 2.7	3.79 ± .12
	.80	.46 ± .02	7.7 ± 0.7	4.14 ± .10
$\frac{p \to \pi^+}{p_T = .3}$	.30	.58 ± .05	9.6 ± 2.0	5.50 ± .26
	.40	.56 ± .02	5.81 ± .51	2.34 ± .19
	.50	.54 ± .03	3.24 ± .38	1.78 ± .17
	.60	.59 ± .05	1.25 ± .26	0.81 ± .05
	.70	.56 ± .07	0.54 ± .14	0.37 ± .03
	.80	.60 ± .11	0.15 ± .07	.062 ± .014
$p_T = .5$	.30	.62 ± .04	3.94 ± .64	2.44 ± .16
	.50	.51 ± .11	1.62 ± .67	0.65 ± .04

	x	α	σ_o	σ_H
$p \to \pi^-$ $P_T = .3$	.30	.62 ± .04	4.28 ± .63	2.71 ± .16
	.40	.53 ± .06	2.60 ± .60	1.31 ± .07
	.50	.56 ± .12	0.72 ± .32	0.48 ± .04
	.60	.52 ± .08	0.41 ± .12	0.25 ± .02
	.70	.55 ± .13	0.09 ± .05	.077 ± .013
$P_T = .5$	.30	.55 ± .04	3.00 ± .51	1.33 ± .12
	.50	.43 ± .08	0.85 ± .25	0.23 ± .03

Figure Captions

Fig. 1 (a)-(i): Invariant cross section per nucleon vs Feynman x measured at $p_T = 0.3$ GeV/c.

Fig. 2 (a)-(f): Invariant cross section per nucleon vs Feynman x measured at $p_T = 0.5$ GeV/c.

Fig. 3 Power $\alpha(x)$ from fits to invariant cross section (per nucleus), $E \frac{d^3\sigma}{dp^3} = \sigma_o A^\alpha$ from Table 2. The curve represents the data of Reference 4 fitted at $p_T = 0.3$ GeV/c.

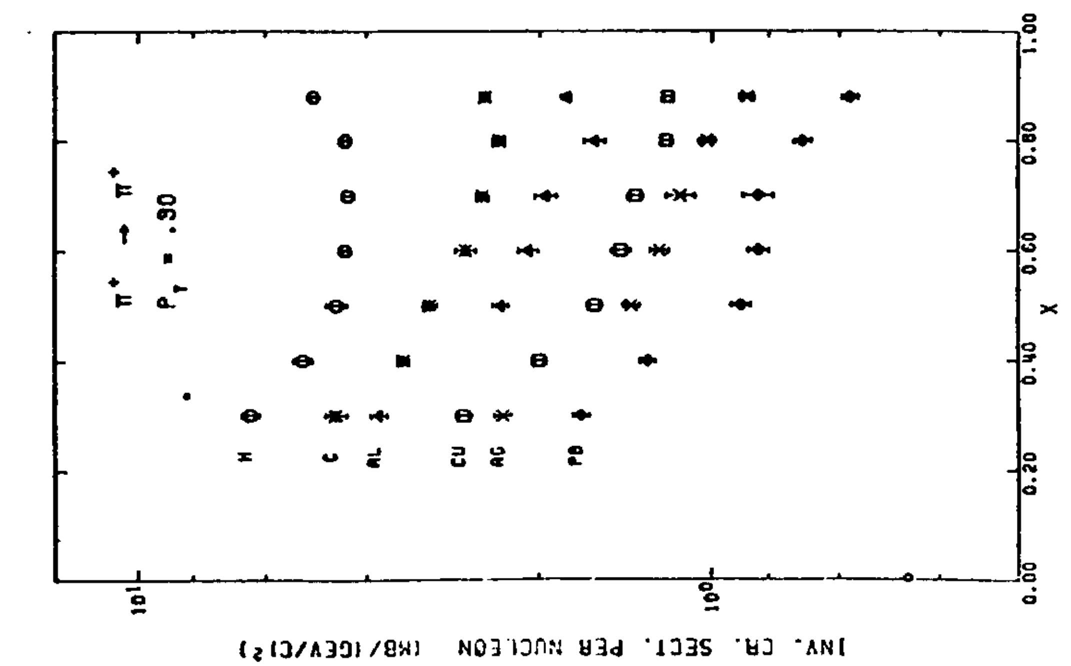
π+ → π+
PT = .30
H
C
AL
CU
AG
PB
X
INV. CR. SECT. PER NUCLEON (MB/(GEV/C)²)
0.00
0.20
0.40
0.60
0.80
1.00

Fig. 1a

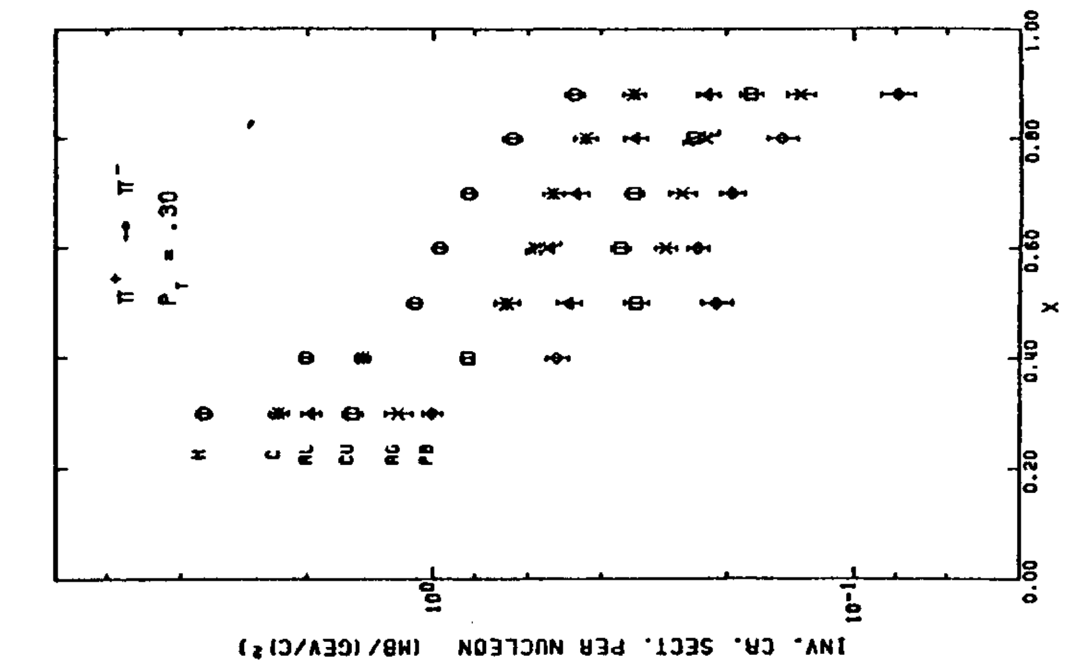
π+ → π−
PT = .30
H
C
AL
CU
AG
PB
X
INV. CR. SECT. PER NUCLEON (MB/(GEV/C)²)
0.00
0.20
0.40
0.60
0.80
1.00

Fig. 1b

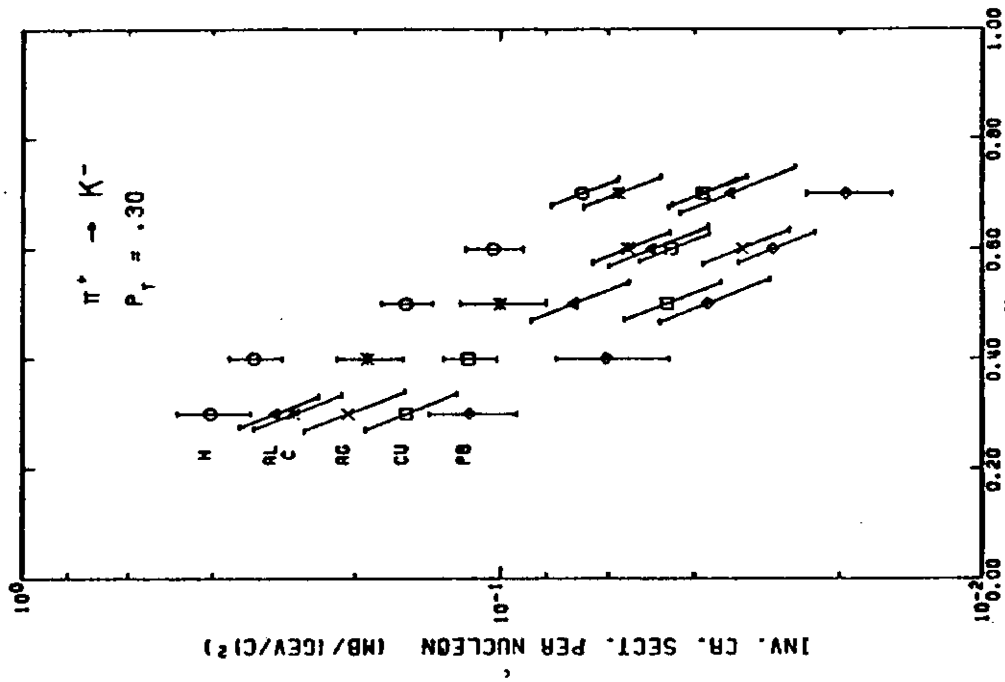
π+ → K−
P_T = .30
H
AL
C
AG
CU
PB
INV. CR. SECT. PER NUCLEON (MB/(GEV/C)²)
X
0.00
0.20
0.40
0.60
0.80
1.00
10^0
10^-1
10^-2

Fig. 1d

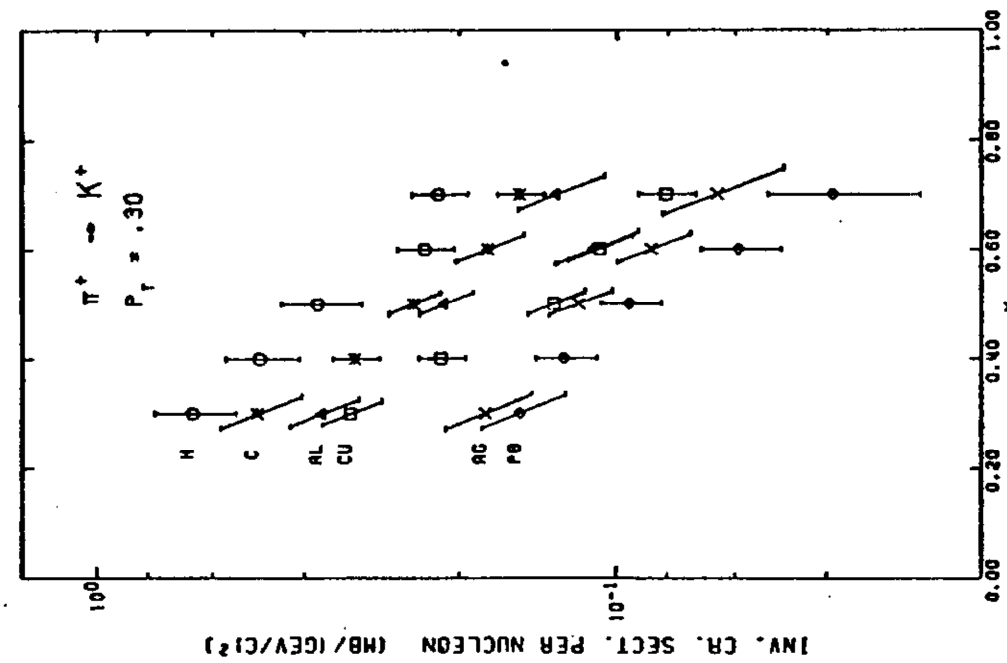
π+ → K+
P_T = .30
H
C
AL
CU
AG
PB
INV. CR. SECT. PER NUCLEON (MB/(GEV/C)²)
X
0.00
0.20
0.40
0.60
0.80
1.00
10^0
10^-1

Fig. 1c

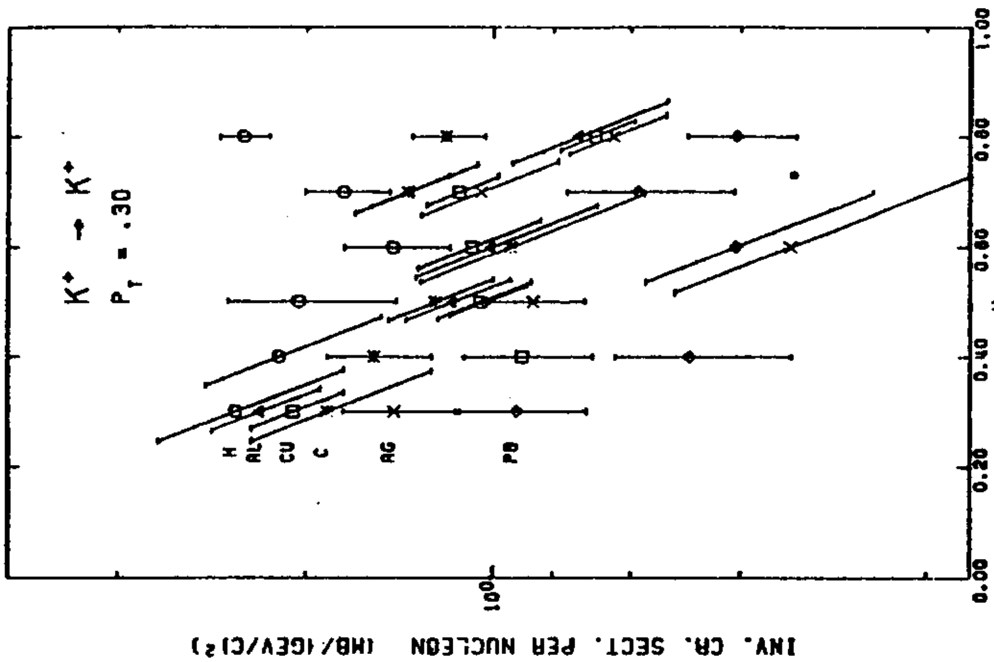
K⁺ → K⁺
P_T = .30
H
AL
CU
C
AG
PB
X
INV. CR. SECT. PER NUCLEON (MB/(GEV/C)²)

Fig. 1f

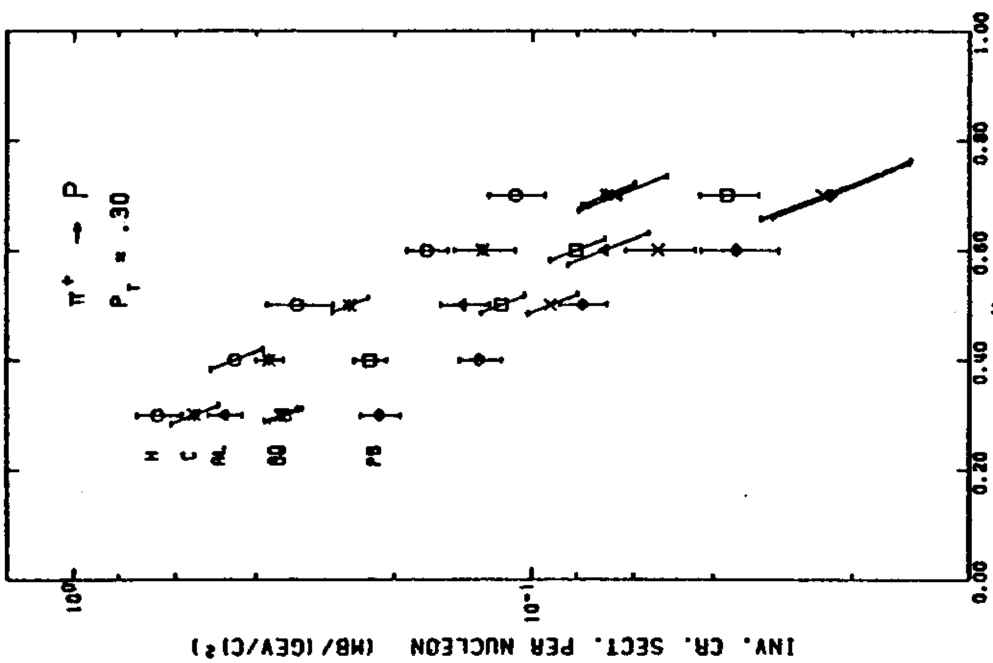
π⁺ → P
P_T = .30
H
C
AL
80
PB
X
INV. CR. SECT. PER NUCLEON (MB/(GEV/C)²)

Fig. 1e

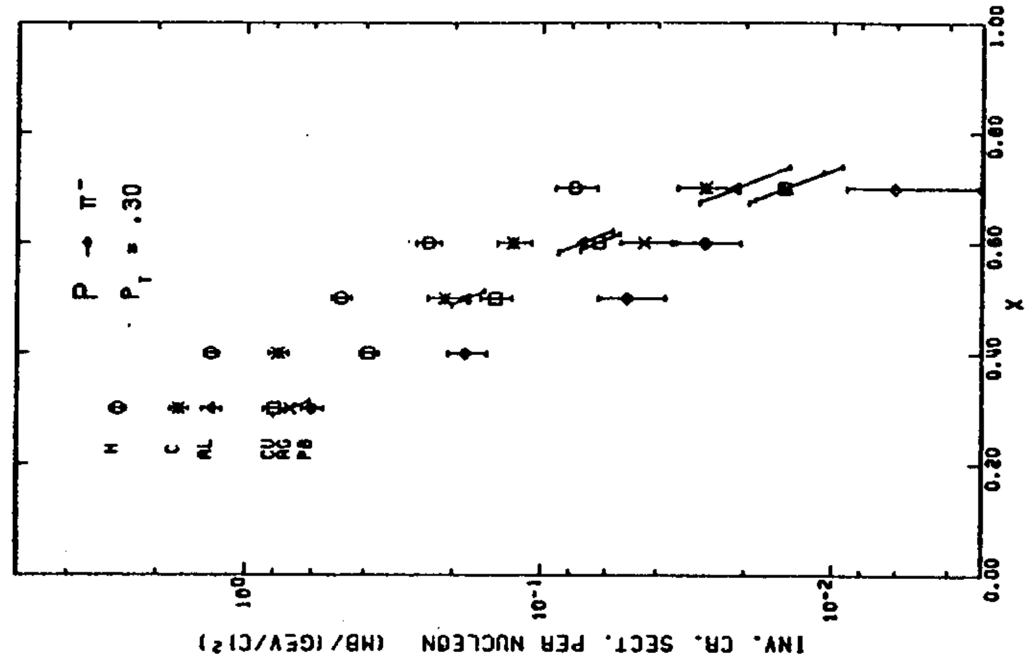

P → π⁻
P_T = .30
H
C
AL
CU
AG
PB
X
INV. CR. SECT. PER NUCLEON (MB/(GEV/C)²)

Fig. 1h

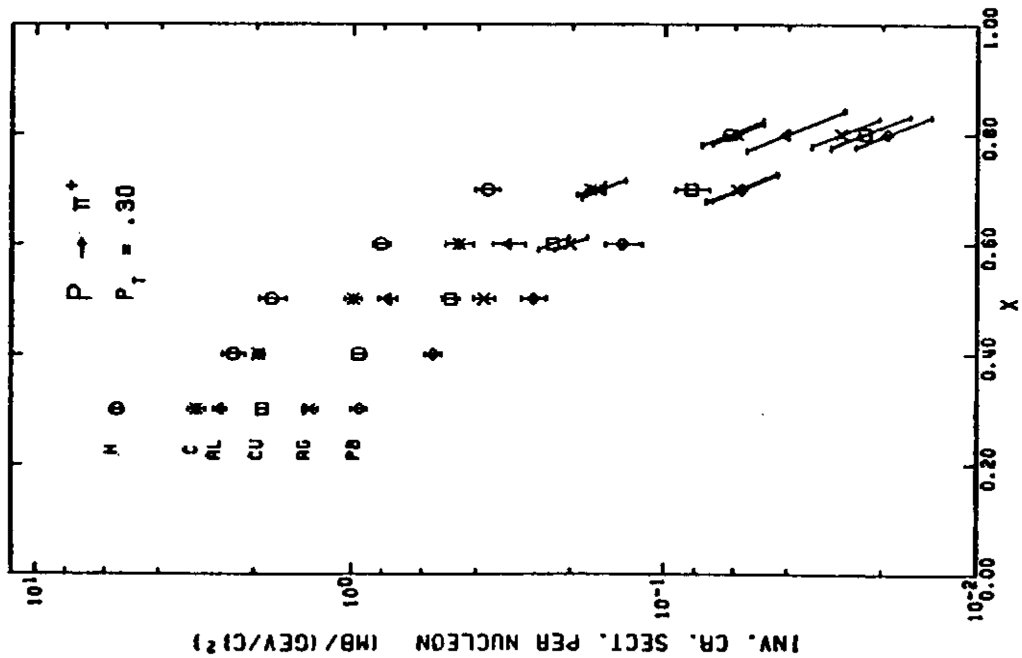

P → π⁺
P_T = .30
H
C
AL
CU
AG
PB
X
INV. CR. SECT. PER NUCLEON (MB/(GEV/C)²)

Fig. 1g

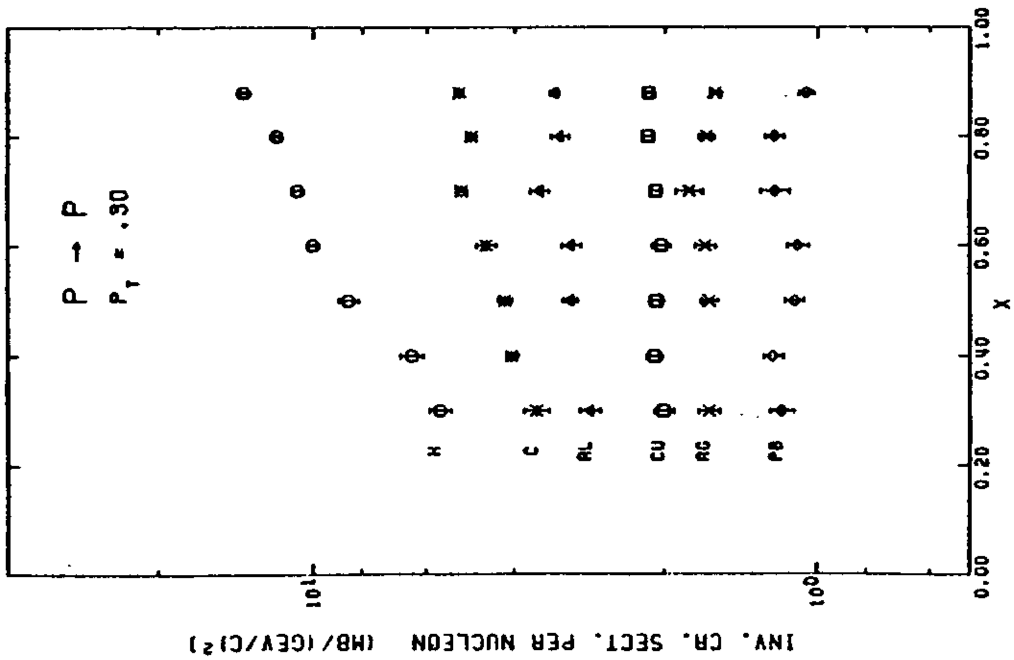
P → P
P_T = .30
H
C
AL
CU
AG
PB
0.00
0.20
0.40
0.60
0.80
1.00
X
10^1
10^0
INV. CR. SECT. PER NUCLEON (MB/(GEV/C)²)

Fig. 11

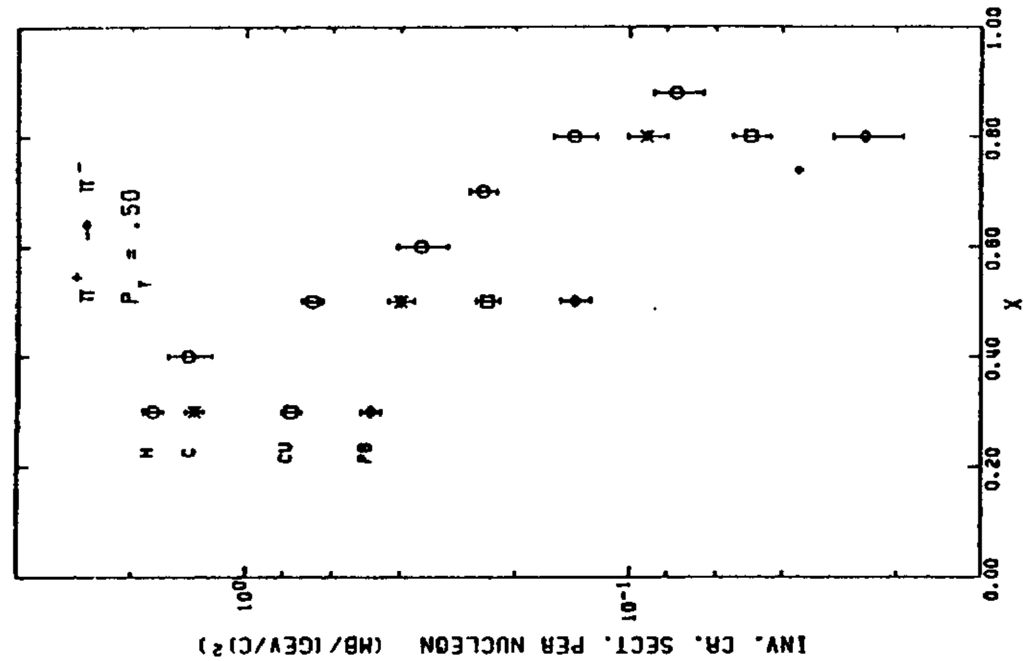
π+ → π−
PT = .50
H
C
CU
PB
X
0.00
0.20
0.40
0.60
0.80
1.00
10^0
10^-1
INV. CR. SECT. PER NUCLEON (MB/(GEV/C)²)

Fig. 2b

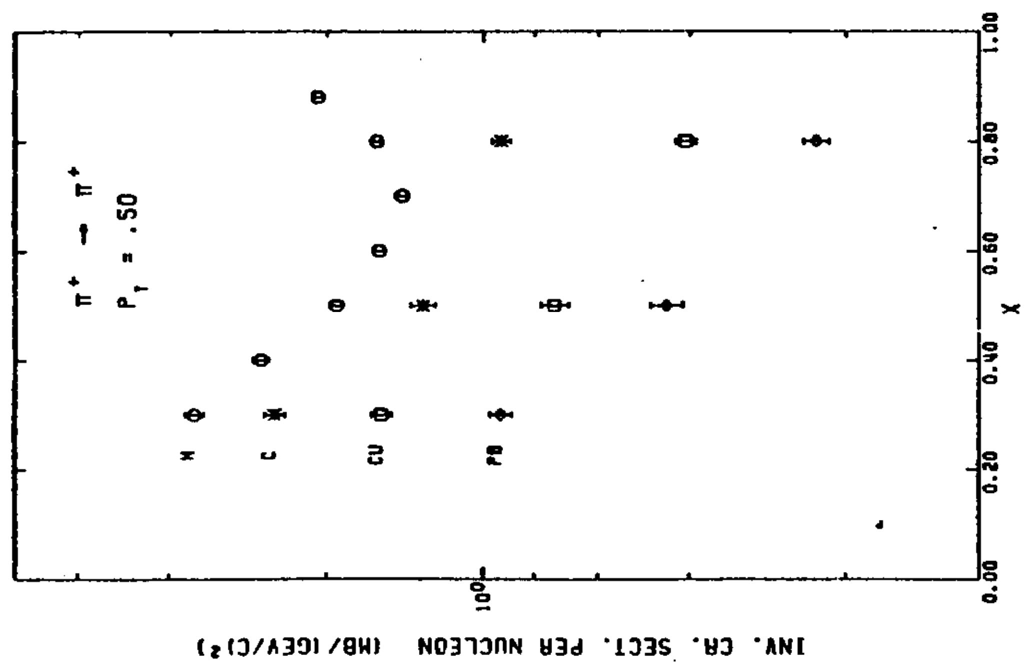
π+ → π+
PT = .50
H
C
CU
PB
X
0.00
0.20
0.40
0.60
0.80
1.00
10^0
INV. CR. SECT. PER NUCLEON (MB/(GEV/C)²)

Fig. 2a

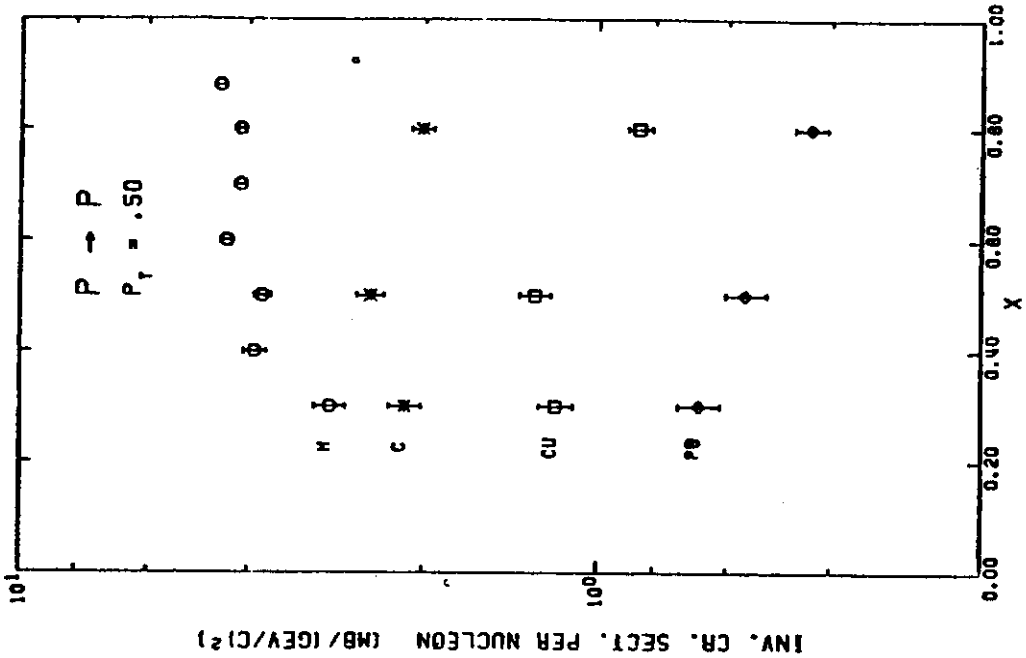
P → P
P_T = .50
H
C
CU
PB
X
INV. CR. SECT. PER NUCLEON (MB/(GEV/C)²)

Fig. 2d

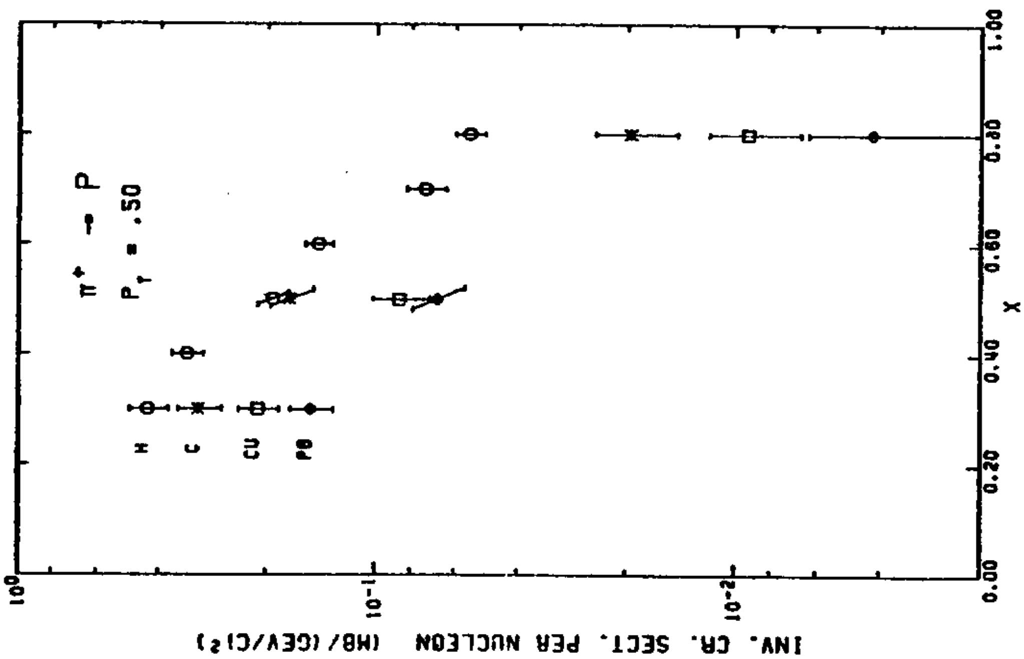
π⁺ → P
P_T = .50
H
C
CU
PB
X
INV. CR. SECT. PER NUCLEON (MB/(GEV/C)²)

Fig. 2c

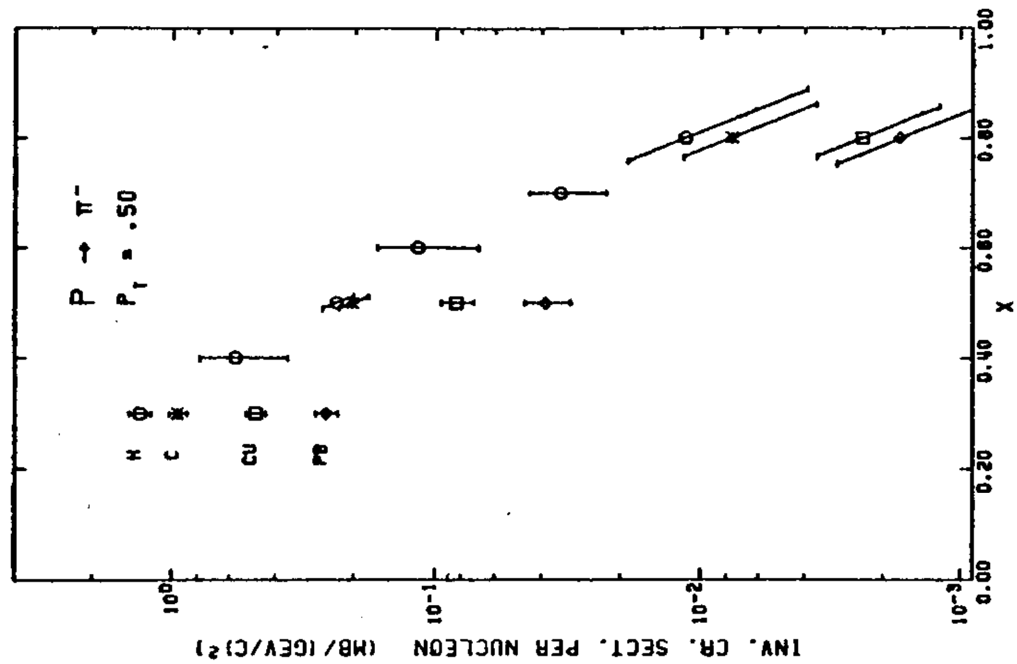
P → π⁻
P_T = .50
H
C
CU
PB
X
INV. CR. SECT. PER NUCLEON (MB/(GEV/C)²)

Fig. 2f

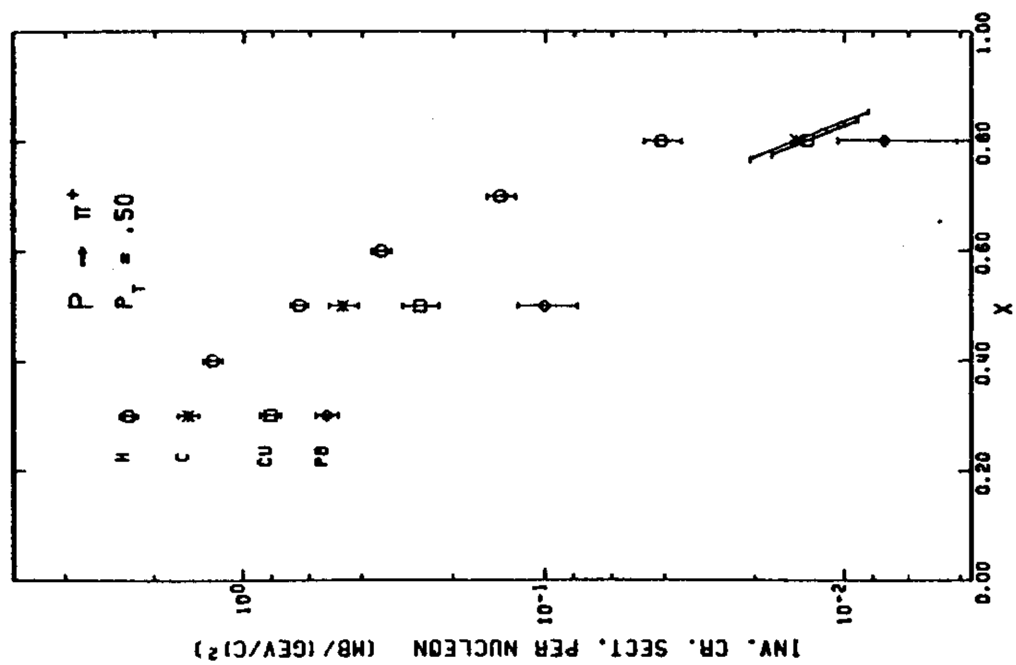
P → π⁺
P_T = .50
H
C
CU
PB
X
INV. CR. SECT. PER NUCLEON (MB/(GEV/C)²)

Fig. 2e

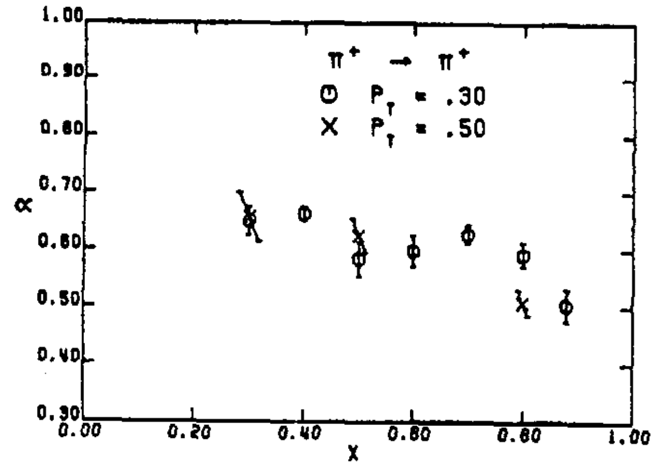

Fig. 3a

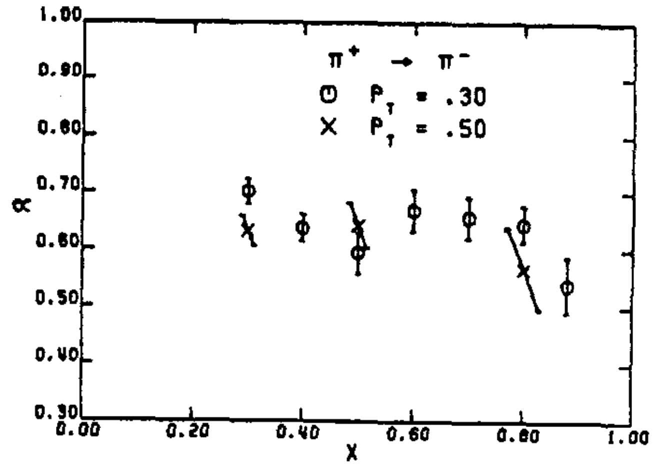

Fig. 3b

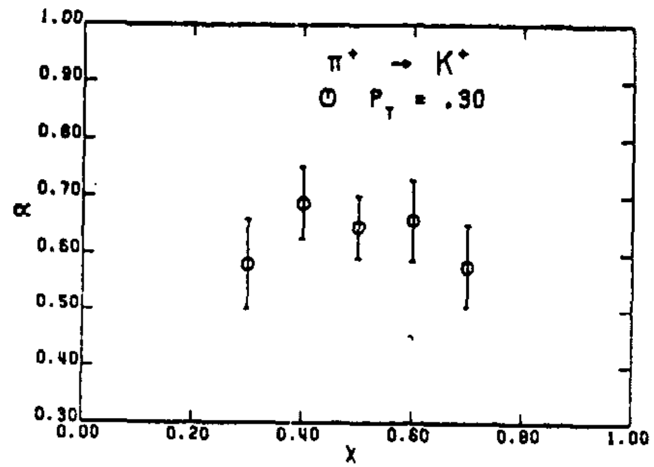

Fig. 3c

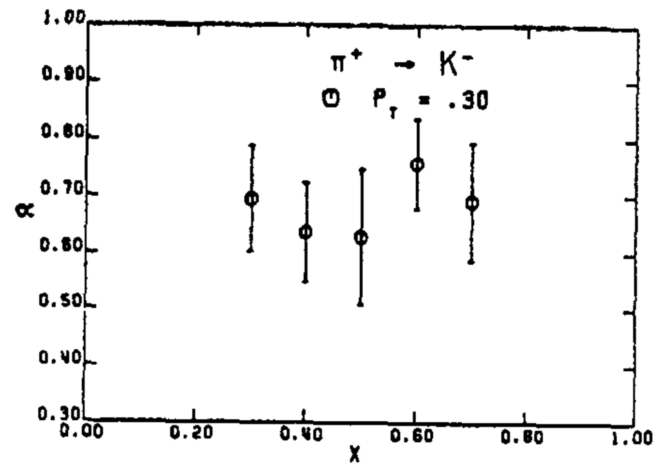

Fig. 3d

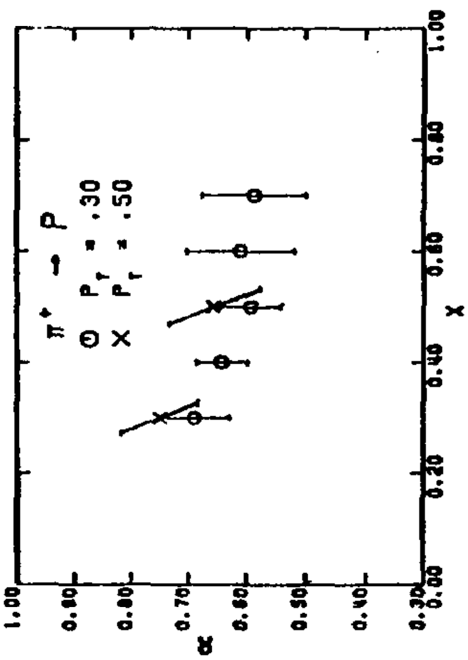

Fig. 3e

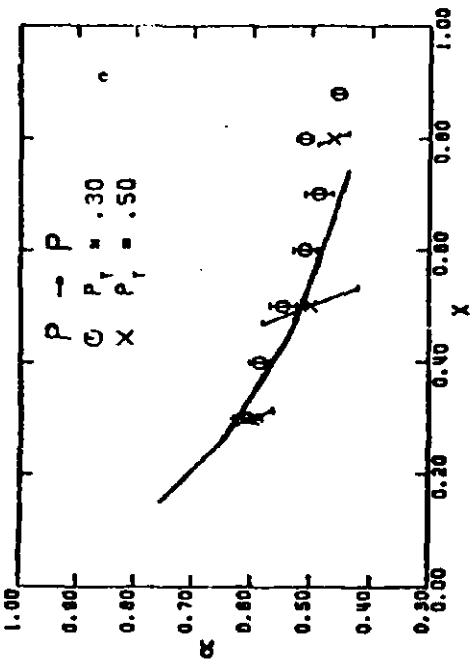

Fig. 3f

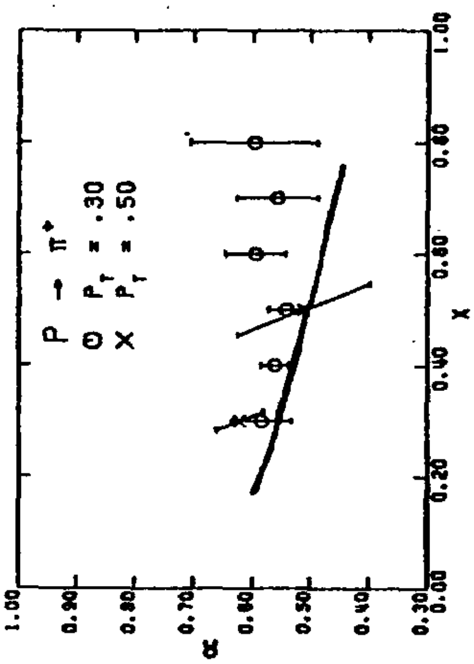

Fig. 3g

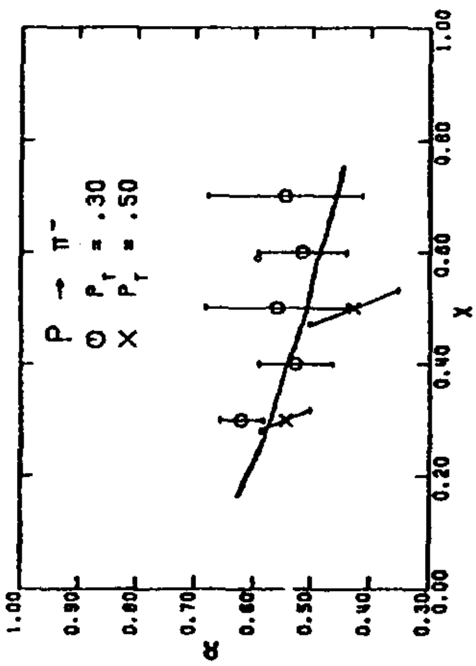

Fig. 3h